POLARON-LIKE VORTICES, DISSOCIATION TRANSITION, AND SELF-INDUCED PINNING IN MAGNETIC SUPERCONDUCTORS

L. N. Bulaevskii[*], *S.-Z. Lin*

Theoretical Division, Los Alamos National Laboratory
87545, Los Alamos, New Mexico, USA

Dedicated to the memory of Professor Anatoly Larkin

Vortices in magnetic superconductors polarize spins nonuniformly and repolarize them when moving. At a low spin relaxation rate and at low bias currents vortices carrying magnetic polarization clouds become polaron-like and their velocities are determined by the effective drag coefficient that is significantly bigger than the Bardeen–Stephen (BS) one. As the current increases, vortices release polarization clouds and the velocity as well as the voltage in the $I–V$ characteristics jump to values corresponding to the BS drag coefficient at a critical current J_c. The nonuniform components of the magnetic field and magnetization drop as the velocity increases, resulting in weaker polarization and a discontinuous dynamic dissociation depinning transition. Experimentally, the jump shows up as a depinning transition and the corresponding current at the jump is the depinning current. As the current decreases, on the way back, vortices are retrapped by polarization clouds at the current $J_r < J_c$. As a result, the polaronic effect suppresses dissipation and enhances the critical current. Borocarbides $(RE)Ni_2B_2C$ with a short penetration length and highly polarizable rare earth spins seem to be optimal systems for a detailed study of vortex polaron formation by measuring $I–V$ characteristics. We also propose to use a superconductor–magnet multilayer structure to study polaronic mechanism of pinning with the goal to achieve high critical currents. The magnetic layers should have large magnetic susceptibility to enhance the coupling between vortices and magnetization in magnetic layers while the relaxation of the magnetization should be slow. For Nb and a proper magnet multilayer structure, we estimate the critical current density $J_c \sim 10^9$ A/m^2 at the magnetic field $B \approx 1$ T.

1. INTRODUCTION

The conception of vortex as a polaron [1] was initiated by experimental data on the critical current in Er borocarbide, and we first discuss these data. The family of quaternary nickel borocarbides $(RE)Ni_2B_2C$ (RE is a rare earth magnetic ion) is an interesting class of crystals that exhibit both singlet superconductivity and magnetic order at low temperatures [2–4]. A number of crystals in that family develop antiferromagnetic order below the Néel temperature T_N, which is below the superconducting critical temperature T_c. Because the spatial periodicity of magnetic moments is well below the superconducting correlation length, superconductivity coexists quite peacefully with the antiferromagnetic order. By contrast, the ferromagnetic order, an-

tagonistic to Cooper pairing, leads to dramatic changes in both magnetic and superconducting orders in the coexistence phase of singlet superconductors (see Ref. [5] for a review).

The compound $ErNi_2B_2C$ with $T_c = 11$ K and $T_N = 6$ K attracted much attention when it was realized that below the phase transition from an incommensurate spin density wave (SDW) to a commensurate SDW at $T^* = 2.3$ K, the phase with a weak ferromagnetic ordering can emerge [6, 7]. It was concluded that the incommensurate SDW develops in $ErNi_2B_2C$ below T_N with effective Ising spins oriented along the a axis and with the wave vector $Q = 0.5526\,b^*$ from neutron scattering measurements [8, 9]. Here, $b^* = 2\pi/b$ and b is the lattice period along the b axis. At T^*, the transition to the commensurate phase with $Q = 0.55b^*$ leaves one out of 20 spins free of the SDW molecular field. These Er spins with the magnetic moment $\mu = 7.8\mu_B$ are easily polarizable by the magnetic field along the a

---

[*]E-mail: lnb@lanl.gov, lnb@viking.lanl.gov

direction. The spin magnetization in the magnetic field $H = 2000$ G in the temperature range 2–4 K follows the law $M_{sp}/H \approx \mu M_s/k_B T$, where $M_s \approx 56$ G (see Fig. 4 in Ref. [7]). The value $M_s = \mu n$ corresponds to the magnetization at which all "free" spins with the concentration n order ferromagnetically. The same value M_s was obtained by extrapolation of the magnetization at the temperature 2 K in fields $H > 1500$ G to $H \to 0$ [10]. Nevertheless, the Hall probe measurements without an applied field below T^* found an internal magnetic field much lower than M_s and no spontaneous vortex lattice was seen [11]. High polarizability of the spin system in $\mathrm{ErNi_2B_2C}$ is a key point of our discussion in what follows.

As the hope to observe remarkable consequences of a weak ferromagnetic phase coexisting with superconductivity waned, the puzzle of the $\mathrm{ErNi_2B_2C}$ critical current behavior at low temperatures remained. It was discovered by measuring the hysteresis in M–H loops and transport measurements that new pinning mechanism develops below 3 K for which the critical current increases as the temperature decreases to ≈ 1.5 K following approximately the enhancement of magnetic susceptibility [10, 12].

To explain these data, the conception of a vortex as a polaron was proposed, i. e., formation of polaron-like vortices dressed by the polarization cloud of magnetic moments [1]. Generally, the polaronic mechanism is inherent to all magnetic superconductors, but it is most pronounced when the magnetic system is highly polarizable, as in the case of $\mathrm{ErNi_2B_2C}$ below 2.3 K. To clarify this mechanism, we recall that the magnetic field is nonuniform within the vortex lattice and is the strongest near the vortex cores. Consequently, the polarization of the magnetic moments is also nonuniform. When vortices move, they should repolarize the magnetic system, otherwise they would lose the energy gained by polarization (the Zeeman energy). The process of repolarization depends on the dynamics of the magnetic system. In what follows, we consider the relaxation dynamics of free spins in $\mathrm{ErNi_2B_2C}$. The repolarization process is controlled by the relaxation time τ that should be compared with the characteristic time a/v needed to shift the vortex lattice moving with the velocity v by the vortex lattice period $a = (\Phi_0/B)^{1/2}$. Here, Φ_0 is the flux quantum, B is the magnetic induction, and we assume a square vortex lattice. For $\tau \gg a/v$, the magnetic moments strongly slow down the vortex motion.

At some critical velocity and critical current J_c, the vortices are stripped off the polarization clouds. The corresponding jump in velocity is more evident for large

τ. As the current decreases, the vortices become re-trapped again at a current $J_r < J_c$. Because the voltage $V \propto v$, the I–V characteristics show hysteresis. The physics here is similar to that of a polaron, with vortices playing the role of electrons and the magnetic polarization the role of phonons [13].

2. GENERAL EQUATIONS

The $\mathrm{ErNi_2B_2C}$ crystals have an orthorhombic structure below T_N with domains where a and b axes change by $90°$ in neighboring domains. We consider a clean single-domain crystal. In multi-domain crystals, the domain walls also provide the pinning of vortices, which is sharply peaked when vortex lines are aligned with the domain walls [14]. We consider the vortex lattice induced by the applied magnetic field $\mathbf{H}$ tilted by an angle θ with respect to the crystal c axis. As revealed by neutron scattering, vortices form a square lattice in $\mathrm{ErNi_2B_2C}$ [15].

We choose the z axis along the direction of vortex lines at rest and the x axis in the ac plane (see Fig. 1). A vortex line deviates from the applied field $\mathbf{H}$ due to the magnetic moments [15]. The system is assumed to be uniform along the direction of vortex lines. In a
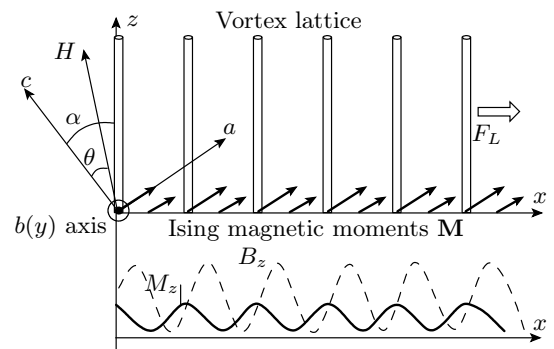

Fig. 1. Schematic view of the vortex lattice in the presence of free Ising magnetic moments along the a axis. The vortex lattice is tilted with respect to the applied magnetic fields in the ac plane due to the polarization of the magnetic moments. The vertical columns show the vortex cores. The polarized magnetic moments are nonuniform in space due to the spatial modulation of the vortex lattice magnetic field. Due to the Lorentz force F_L, vortices move along the x axis. In the moving lattice, there is a phase shift between the magnetic induction B_z (dashed line) associated with the vortex lattice and the magnetization M_z (solid line) caused by the retardation in the response of magnetic moments to the vortex magnetic field

static situation, the direction of vortex lines is determined by the effective field $\mathbf{H} + 4\pi\overline{\mathbf{M}}$, where $\overline{\mathbf{M}}$ is the spatial average of the magnetization. We let α denote the angle between vortex lines and the c axis.

The Lagrangian $\mathcal{L}\{\mathbf{R}_i(t), M_z(\mathbf{r}, t)\}$ for the whole system is given by

$$\mathcal{L}\{\mathbf{R}_i(t), M(\mathbf{r}, t)\} = \mathcal{L}_M\{M_z(\mathbf{r}, t)\} + \mathcal{L}_v\{\mathbf{R}_i(t)\} + $$
$$+ \mathcal{L}_{int}\{M_z(\mathbf{r}, t), \mathbf{R}_i(t)\} + \mathcal{L}_{vv}\{\mathbf{R}_i\} + \mathcal{L}_F\{\mathbf{J}\}, \quad (1)$$

where

$$\mathcal{L}_M\{M_z(\mathbf{r}, t)\} = -\int d\mathbf{r} \frac{M_z^2(\mathbf{r}, t)}{2\chi_{zz}} \quad (2)$$

is the Lagrangian for the magnetic subsystem and

$$\mathcal{L}_v\{\mathbf{R}_i(t), \mathbf{r}_j\} = -\sum_{i,j} U(\mathbf{R}_i - \mathbf{r}_j) \quad (3)$$

is the Lagrangian for the interaction between vortices and the pinning potential due to quenched disorder. Here, $U(\mathbf{R}_i - \mathbf{r}_j)$ is the pinning potential at $\mathbf{r}_j$. Further, $\mathcal{L}_{vv}\{\mathbf{R}_i\}$ is the vortex–vortex interaction,

$$\mathcal{L}_F\{\mathbf{J}\} = \sum_i \mathbf{J} \cdot \mathbf{R}_i \frac{\Phi_0}{c}$$

is the Lagrangian due to the Lorentz force in the presence of a bias current density $\mathbf{J}$, and χ_{zz} is the magnetic susceptibility at the working external magnetic field. It describes response of magnetic moments to the nonuniform component of the field induced by vortices.

In the London approximation, the magnetic field of the vortex lattice inside the crystal is ($\mathbf{r} = x, y$)

$$B_z(\mathbf{r}) = \bar{B}_z \sum_{\mathbf{G}} \frac{\cos(\mathbf{G} \cdot \mathbf{r})}{\lambda^2 \mathbf{G}^2 + 1}, \quad (4)$$

where $\bar{B}_z$ is the averaged magnetic induction, $\mathbf{G}$ are reciprocal vectors of the square lattice, and λ is the superconducting penetration length renormalized by the magnetic moments. It is given by the expression $\lambda^2 = \lambda_L^2(1 - 4\pi\chi_{zz})$, where λ_L describes magnetic field penetration in the absence of the magnetic moments [5, 16–19]. We note that the magnetic susceptibility $\chi_{zz} = M_z/B_z$ is smaller than $1/4\pi$, i. e., $\chi_{zz} < 1/4\pi$. The magnetic fluctuations $\langle M_z M_z \rangle \sim \chi_{zz}/(1 - 4\pi\chi_{zz})$ diverge as $\chi_{zz} \to 1/4\pi$, which indicates instability of the magnetic system [20]. We here also ignore anisotropy of the penetration length.

In the Lagrangian, the interaction between a vortex line at $\mathbf{R}_i = (x_i, y_i)$ and the magnetic moments is determined by the term

$$\mathcal{L}_{int}\{\mathbf{R}_i, \mathbf{M}_z\} = \int dt \int d\mathbf{r} B_z(\mathbf{R}_i - \mathbf{r}, t) M_z(\mathbf{r}, t), \quad (5)$$

where we describe the magnetic moments in the continuous approximation via the magnetization $M_z(\mathbf{r}, t)$, because the distance between free spins, equal to 35 nm [9] is much smaller than the London penetration length λ, about 500 nm [15]. We ignore the pair breaking effect of the magnetic moments because they suppress Cooper pairing uniformly as the distance between free spins is much smaller than the coherence length, and hence the pair breaking effect by the moments does not introduce pinning.

Both the magnetization and vortices are governed by a relaxation dynamics characterized by the dissipation function

$$\mathcal{R}\{\mathbf{R}_i(t), M_z(\mathbf{r}, t)\} = \mathcal{R}_{M_z} + \mathcal{R}_v,$$

where

$$\mathcal{R}_{M_z}\{\dot{M}_z(\mathbf{r})\} = \frac{1}{2}\tau \int d\mathbf{r} \dot{M}_z^2(\mathbf{r}),$$
$$\mathcal{R}_v\{\dot{\mathbf{R}}_i\} = \eta \sum_i \frac{1}{2} \dot{\mathbf{R}}_i^2. \quad (6)$$

Here, τ is the relaxation time for a single spin and $\eta = \Phi_0^2/2\pi\xi^2 c^2 \rho_n$ is the Bardeen–Stephen drag coefficient per unit vortex length with ρ_n being the normal resistivity slightly above T_c. The equation of motion for vortices is the Euler-Lagrange equation of motion

$$\frac{d}{dt}\frac{\delta\mathcal{L}}{\delta\dot{\mathbf{R}}_i} - \frac{\delta\mathcal{L}}{\delta\mathbf{R}_i} + \frac{\delta\mathcal{R}}{\delta\dot{\mathbf{R}}_i} = 0, \quad (7)$$

which gives

$$\eta\frac{\partial\mathbf{R}_i}{\partial t} = \frac{\partial\mathcal{L}_{vv}\{\mathbf{R}_i, \mathbf{R}_j\}}{\partial\mathbf{R}_i} + \frac{\partial\mathcal{L}_{int}\{\mathbf{R}_i, \mathbf{M}\}}{\partial\mathbf{R}_i} +$$
$$+ \sum_j \frac{\partial U(\mathbf{R}_i - \mathbf{r}_j)}{\partial\mathbf{R}_i} + \mathbf{F}_L, \quad (8)$$

with $\mathbf{F}_L = \Phi_0\mathbf{J}/c$ being the Lorentz force.

We here neglect the effect of quenched disorder because the vortex motion quickly averages out the disorder and the lattice ordering is improved [21, 22]. In the lattice phase, $\mathcal{L}_{vv} = 0$ due to symmetry. The equation of motion for vortex lines is then

$$\eta\frac{\partial\mathbf{R}_i}{\partial t} = \frac{\partial\mathcal{L}_{int}\{\mathbf{R}_i, M_z\}}{\partial\mathbf{R}_i} + \mathbf{F}_L. \quad (9)$$

The magnetization dynamics is governed by

$$\tau\frac{\partial M_z(\mathbf{r}, t)}{\partial t} = -\left[\frac{M_z(\mathbf{r}, t)}{\chi_{zz}} - B_z(\mathbf{r})\right]. \quad (10)$$

It follows from Eq. (10) that the relaxation time of the magnetization measured experimentally in the crystal

is $\chi_{zz}\tau$. The force due to magnetic moments is the same for all lines and the vortex lattice moves as a whole. The motion of the vortex lattice center of mass, $u(t)$, along the x axis is described by the equation

$$\eta\frac{\partial u}{\partial t} = \frac{\partial}{\partial u}\left[\int d\mathbf{r}B_z(x+u,y,t)M_z(\mathbf{r},t)\right] + F_L. \quad (11)$$

Using the linear response approach to relate magnetization to the magnetic field, we obtain

$$\eta\frac{\partial u}{\partial t} = \frac{\partial}{\partial u}\int d\mathbf{r}d\mathbf{r}'B_z(x+u,y,t) \times$$
$$\times \int_0^t dt'\chi_{zz}(\mathbf{r}-\mathbf{r}',t-t')B_z(\mathbf{r}',t') + F_L. \quad (12)$$

The vortex lattice moves with the constant velocity $u = vt$ in the steady state $t \gg \tau$. Integrating over coordinates and time, we obtain

$$\eta v = \sum_{\mathbf{G}}\frac{\chi_{zz}(\mathbf{G},\mathbf{v}\cdot\mathbf{G})}{(\lambda^2\mathbf{G}^2+1)^2} + F_L, \quad (13)$$

where $\chi_{zz}(\mathbf{k},\omega)$ is the dynamic magnetic susceptibility in the Fourier representation. We see that the magnetic moments affect the vortex motion strongly if either a) the resonance Cherenkov radiation condition $\mathbf{v}\cdot\mathbf{G} = \Omega(\mathbf{G})$ is fulfilled, where $\Omega(\mathbf{k})$ is the frequency of magnetic excitations with the momentum $\mathbf{k}$ and $\Omega(\mathbf{k}) \gg \Gamma(\mathbf{k})$, where $\Gamma(\mathbf{k})$ is the relaxation rate of the excitation, or b) dynamics of the magnetic system is dominated by relaxation, $\Omega(\mathbf{k}) \lesssim \Gamma(\mathbf{k})$. In the former case, discussed in Refs. [23–25], the magnetic moments renormalize the vortex viscosity at high velocities when the alternating magnetic field of vortices is able to excite magnons. Here, we consider the latter case of free moments described by the relaxation dynamics according to Eq. (10) with $\chi_{zz}(\mathbf{k},\omega)$ given by

$$\chi_{zz}(\mathbf{k},\omega) = \chi\sin^2\alpha\frac{1}{1-i\omega\tau\chi}, \quad \chi = \frac{\mu M_s}{k_BT}, \quad (14)$$

at temperatures T below 3 K for $ErNi_2B_2C$.

Renormalizing time in units of $\tau\chi$, length in unit of $1/G_1$, force per unit vortex length in unit of $\eta/\tau G_1\chi$ we obtain the equation for velocity

$$v + F_p\frac{v}{v^2+1} = F_L, \quad (15)$$

where we take only the dominant lattice wave vector $\mathbf{G}_1 = (2\pi/a, 0, 0)$ into account and introduce the magnetic pinning force per unit vortex length

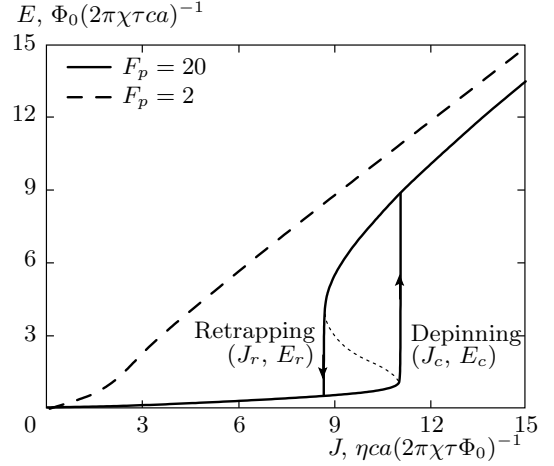$$F_p = \frac{\Phi_0^2\tau\chi^2\sin^2\alpha}{4\pi^2\lambda^4\eta}.$$

Fig. 2. Calculated I–V curves for $F_p = 20$ and $F_p = 2$. For $F_p = 20$, the system shows hysteresis in the I–V curve, while for $F_p = 2$, no hysteresis is present. The dotted line denotes the unstable solution
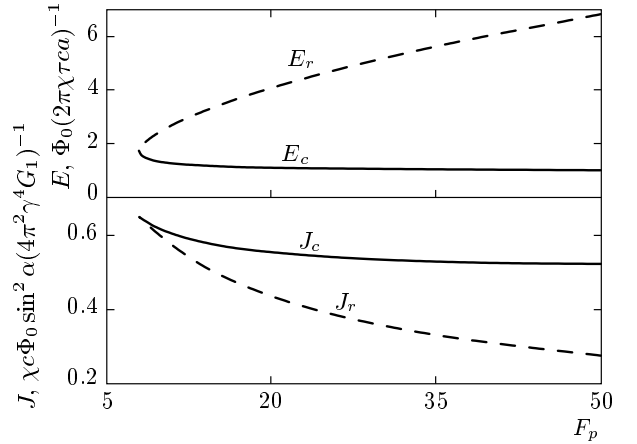

Fig. 3. Dependence of the critical current J_c and retrapping current J_r, and the corresponding electric fields E_c and E_r, on F_p. When $F_p < 8$, hysteresis in the I–V curve disappears

At a low bias current (low F_L), the velocity is proportional to F_L, but with an enhanced effective viscosity, $v \approx F_L/(1+F_p)$. At large F_L (large v), the renormalization disappears and the I–V characteristic becomes the usual Bardeen–Stephen one. Importantly, at $F_p > 8$, the change occurs through a sharp transition, as is shown in Fig. 2. Equation (15) at $F_p > 8$ for an intermediate J has three real solutions: the largest v_3 corresponds to decoupled motion of the vortex lattice and magnetization, the smallest v_1 corresponds to the vortex–polaron motion, and the intermediate solution v_2 corresponds to an unstable state.

The jump at J_c, identified experimentally as the depinning transition, is caused by the dissociation of the vortex–magnon polaron. It is very similar to the dissociation of the usual electron–phonon polaron in high electric fields, as is described theoretically in [26] and confirmed experimentally in metal oxides in [27]. Upon decreasing the current, the vortices are retrapped by the polarization clouds at a threshold current J_r and the vortex lattice moves with a significantly enhanced viscosity at lower currents. The calculated J_c and J_r and the corresponding electric fields are shown in Fig. 3. At large F_p, the critical current is independent of τ,

$$ J_c \approx 0.03 \frac{\chi c \Phi_0 \sin^2 \alpha}{G_1 \lambda^4}, \tag{16} $$

J_c decreases with the temperature as $J_c \sim 1/T$, and decreases with the magnetic field as $J_c \sim 1/\sqrt{B}$.

We explain the origin of the jumps at J_c and J_r. The dependence of the magnetization on the velocity of moving vortices is

$$ M_z(\mathbf{r}, v, t) = \chi \bar{B} \sin^2 \alpha \times $$
$$ \times \sum_{\mathbf{G}} \frac{\cos[\mathbf{G} \cdot \mathbf{r} - \beta(v)]}{(\lambda^2 \mathbf{G}^2 + 1)[1 + (G_1 v \tau \chi)^2]^{3/2}} \tag{17} $$

with $\mathrm{tg}\,\beta = G_1 v \tau \chi$. The nonuniform component of the magnetization and hence the polarization effect decrease with velocity. On the other hand, the retardation between the magnetic field and the magnetization, described by the phase shift $\beta(v)$, increases with the velocity. This positive feedback and the increase in retardation with velocity ensure discontinuous transitions at J_c and J_r.

3. DISCUSSION OF EXPERIMENTAL DATA FOR ERBIUM BOROCARBIDE

A large parameter F_p is required to have a strong pinning due to the polaron mechanism. It is expressed in terms of τ as $F_p \approx 10^{11} \chi \tau \sin^2 \alpha \; \mathrm{s}^{-1}$, where we use the coherence length $\xi \approx 13$ nm [15] and the normal resistivity $\rho_n = 5 \; \mu\Omega \cdot$cm at T_c [28]. The relaxation rate $\chi\tau$ in $\mathrm{ErNi_2B_2C}$ is long because the dynamics of majority of spins is strongly suppressed by the formation of the SDW molecular field, as was found by the Mössbauer measurements in [29]. The relaxation rate drops very fast below 10 K and reaches the value $\chi\tau \approx 5 \cdot 10^{-10}$ s at $T = 5$ K. The data at lower temperatures were not measured, however. Hence, the only information we have so far is $F_p > 50 \sin^2 \alpha$.

The critical current for $\mathrm{ErNi_2B_2C}$ reported in Ref. [10] is about 250 A/cm^2 for $B = 0.1$ T and $T = 2$ K, which corresponds to $\alpha = 2.5°$ according to Eq. (16). The applied magnetic field was close to the c axis in experiment, but the precise angle θ was not reported [10]. The estimate of the order of $1°$ is reasonable, but the quantitative comparison is not convincing because we do not know τ and therefore F_p below 2.3 K. We predict hysteretic behavior in $\mathrm{ErNi_2B_2C}$, a strong dependence of the voltage and of the critical current on the angle θ, at least for $\theta \gg 0.15°$. Hence, the real check of the polaronic mechanism should be by measuring the I–V characteristics. We estimate that the critical current reaches values as high as 10^6 A/cm^2 at large angles at $T = 1$ K and $B = 0.1$ T.

The effect of ordered spins on the vortex motion is similar to that described in Refs. [23–25] for an antiferromagnet. When the Cherenkov radiation condition $\mathbf{v} \cdot \mathbf{G} = \Omega(\mathbf{G})$ is satisfied, excitation of magnons results in an enhanced drag coefficient by transferring energy from vortex motion to the magnetic subsystem. This occurs at high velocities (high currents) of vortices, due to a gap in the magnon spectrum and a large velocity of a magnon, leading to a voltage drop in comparison with the bare Bardeen–Stephen (BS) result.

In the incommensurate SDW with $T > T^*$, some spins experience a quite weak SDW molecular field. Hence, they are polarized by vortices and exhibit the polaronic effect and pinning. This accounts for the increase in pinning in $\mathrm{ErNi_2B_2C}$ as T decreases below T_N (see Ref. [10]), and also the pinning in the holmium borocarbide below T_N [30].

We next discuss the effect of quenched disorder. In the presence of quenched disorder, the vortex lines adjust themselves to take the advantage of the pinning potential, which destroys the long-range lattice order. Below a threshold current, vortices remain pinned (they actually creep between pinning centers due to fluctuations) and the polaronic mechanism does not play a role in that region. When the current is high enough to depin the vortices from quenched disorder, vortices start to move and the lattice ordering is improved. The vortex viscosity is enhanced by formation of a polaron with a nonuniformly induced magnetization. The polaron dissociates and the system jumps to the conventional BS branch at a critical velocity (current). Pinning due to quenched disorder works in the static region and the polaronic pinning works in the dynamic region. The critical current of the whole system is therefore the sum of these two threshold currents. We note that magnetostriction in combination with quenched disorder enhance the polaronic pinning mechanism.
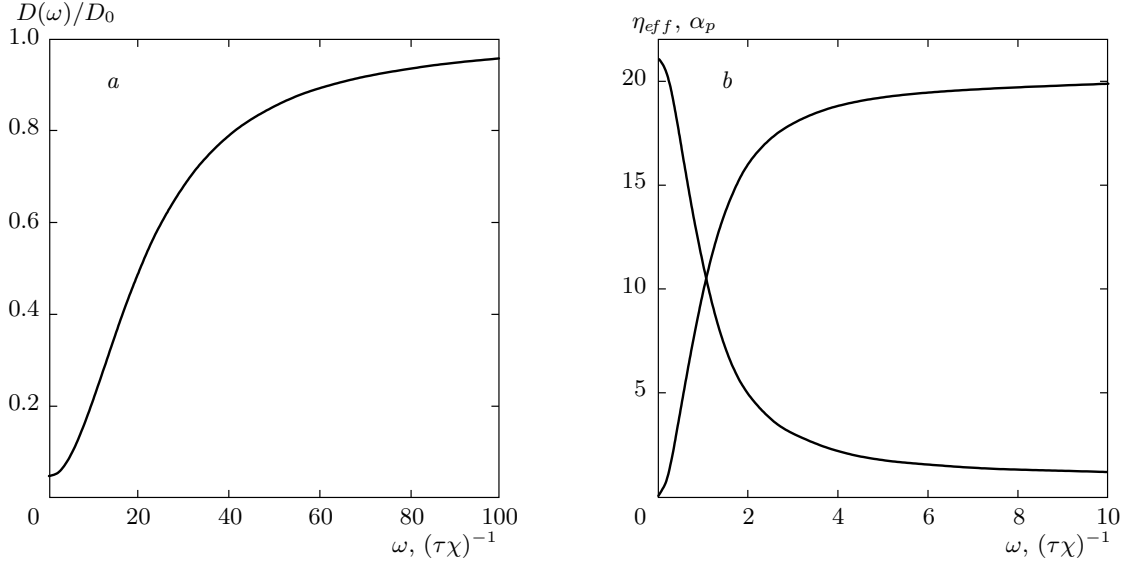
Fig. 4. Dependence of (*a*) the normalized dissipation power $D(\omega)/D_0$, and (*b*) the effective viscosity η_{eff} (lower curve at right) and the pinning strength α_p on the driving frequency ω in the linear regime $F_{ac} \ll \omega(1 + F_p)$. Here, $F_p = 20$

4. RESPONSE OF THE VORTEX LATTICE TO AN *ac* DRIVING CURRENT

Here, we study the response of a vortex polaron to an *ac* driving current [31]. We write the equations of motion for the magnetization

$$m(t) = M(G_1, t)\lambda^2 G_1^2 / \Phi_0 \chi$$

and the vortex lattice center of mass $u(t)$ as

$$\partial_t m(t) = -[m(t) - \exp(-iu(t))], \qquad (18)$$

$$\partial_t u = F_L - \text{Im}\,[F_p \exp(iu)m(t)], \qquad (19)$$

with an *ac* Lorentz force $F_L = F_{ac} \sin(\omega t)$. Eliminating $m(t)$, we obtain the equation for $u(t)$:

$$\frac{du}{dt} = F_L - F_p \int_0^t dt' \sin[u(t) - u(t')] \exp(t' - t). \qquad (20)$$

We first consider the *ac* current regime with a low amplitude $F_{ac}/[\omega(1 + F_p)] \ll 1$. Then the vortex lattice oscillates, $u = \text{Re}[u_{ac} \exp(i\omega t)]$, with the amplitude

$$u_{ac} = F_{ac}(i\eta_{eff}\omega + \alpha_p)^{-1}, \qquad (21)$$

$$\eta_{eff} = 1 + F_p(\omega^2 + 1)^{-1}, \quad \alpha_p = F_p \omega^2(\omega^2 + 1)^{-1}. \quad (22)$$

For a high frequency $\omega \gg 1$, the effect of magnetization is to introduce the pinning potential $U_M = F_p u^2/2$

with the strength F_p. In this case, the vortex lattice follows the driving force much faster than the magnetization does, which remains almost time independent. The polarization of the magnetization results in a periodic pinning potential with the vortex lattice periodicity because it was induced by the same lattice at previous positions and previous instants of time. For a low frequency $\omega \ll 1$, the effect of magnetization is to renormalize the drag coefficient from η to $\eta_{eff} = 1 + F_p$. In this polaron region, the magnetization follows vortex motion by formation of a vortex polaron, as in the *dc* case $\omega = 0$, resulting in the enhancement of viscosity and suppression of *ac* dissipation.

The dissipation power of the whole system, averaged over time, $D(\omega) = \langle F_L(t)v(t)\rangle_t$, is reduced due to the presence of magnetic moments. In the linear region with a vortex polaron, we obtain

$$D(\omega) = \frac{F_{ac}}{2} \frac{\omega^2 \eta_{eff}}{\alpha_p^2 + \eta_{eff}^2 \omega^2}. \qquad (23)$$

This dissipation power should be compared with that the case without magnetic moments (at $F_p = 0$), $D_0 = F_{ac}^2/2$. For $\omega \gg 1$, we have $D/D_0 \approx 1$ and for $\omega \ll 1$, we have $D/D_0 = (1 + F_P)^{-1}$. The frequency dependence of the normalized dissipation power $D(\omega)/D_0$, the effective viscosity η_{eff}, and the pinning strength α_p is shown in Fig. 4. The dissipation of the system in the presence of the magnetic subsystem is strongly reduced in the linear regime $F_{ac} < F_{Lc}$, which might be useful for applications.

We next consider larger driving force amplitudes. In this hysteretic regime, we describe the system analytically in the adiabatic limit, $\omega \ll 1$. At the time instant t_c, when $F_L(t) = F_{Lc} \approx 0.5 F_p$, polaron dissociation leaves the magnetization and the vortex lattice weakly coupled because the lattice now moves with a high velocity. The magnetization component $m(t)$ after that instant relaxes as $m(t) = \exp(-t + t_c)$, and motion of the vortex lattice is determined by the equation

$$\frac{du}{dt} = F_{Lc} + F_p \sin u \exp(-t + t_c). \qquad (24)$$

When $t - t_c < 1$, the vortex lattice velocity oscillates with the frequency $\Omega = F_{Lc}$,

$$v = F_{Lc} + F_p \sin(F_{Lc} t) \exp(-t + t_c), \qquad (25)$$

but the oscillations relax on the time scale of unity. These post-dissociation oscillations are caused by the motion of the vortex lattice in the periodic potential induced by the remnant retarded magnetization.

To take both the retardation and nonlinearity into account for an arbitrary ω, we solve Eqs. (18) and (19) numerically. We consider the interesting region $F_p > 8$, where the dissociation of a vortex polaron is possible due to nonlinear effects at $u \geq 1$. We set $F_p = 20$ in the discussion in what follows. The hysteretic behavior of the vortex lattice velocity vs. the driving force is shown in Fig. 5. At frequencies $\omega \lesssim 1$, which are similar to the dc case $\omega = 0$, we see the following sequence of events during the period of $F_L(t)$: polaron formation near low $|F_L|$ (the interval of low vortex velocity); polaron dissociation (a sharp increase in velocity) followed by the region of vortex oscillations on the background of the average high velocity; a decrease in velocity as the Lorentz force drops and vortex retrapping (a sharp drop in the vortex velocity); and, again, dissociation at a negative $-F_{Lc}$ (a sharp drop in velocity). The results for the behavior of the vortex velocity in time, $v(t)$, are shown in Fig. 6 at $F_{ac} = 20 > F_{Lc}$ and different ω.

At all frequencies $\omega \lesssim 1$, we see post-dissociation oscillations caused by the motion of decoupled vortices with respect to the periodic potential created by the nonuniform magnetization induced by the same lattice just before decoupling (when the velocity was still low) and frozen for some period of time after decoupling due to the retardation effect. This self-induced pinning due to the retardation, and the amplitude of corresponding vortex oscillations reach a maximum at $\omega \approx 1$. In a rough approximation, we describe them by the equation

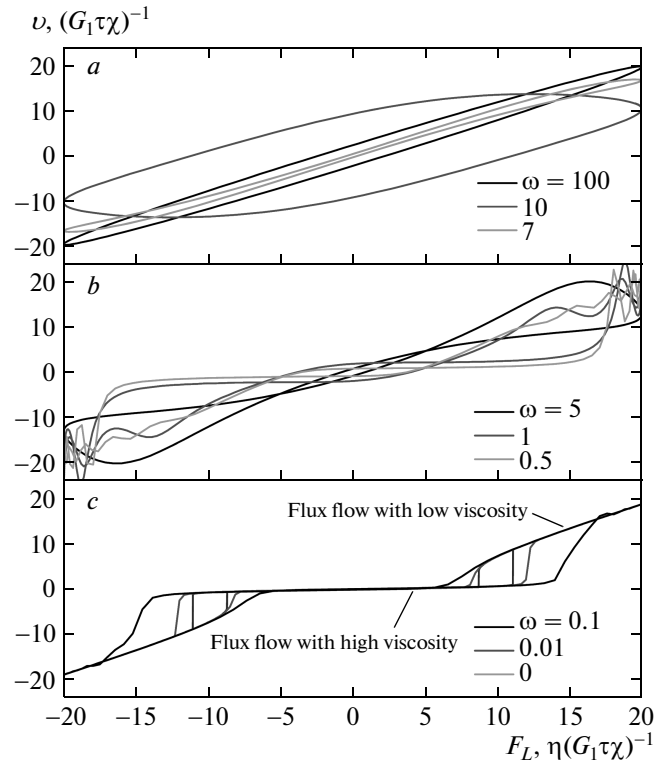$$\frac{du}{dt} \approx F_{Lc} + F_p m_d \sin(u - u_d), \qquad (26)$$

Fig. 5. Dependence of the vortex velocity $v(t)$ on the driving force $F_L(t) = F_{ac}\sin(\omega t)$ with $F_{ac} = 20$. Here, $F_p = 20$

assuming approximately constant m and $F_L = F_{Lc}$ in the regions of maxima and minima of the Lorentz force. Here, u_d and m_d are the vortex lattice position and the magnetization amplitude at the instant of decoupling. This gives the approximate solution

$$v(t) \approx F_{Lc} + F_p m_d \sin(F_{Lc} t), \qquad (27)$$

which provides rough estimate for the oscillation frequency $\Omega \approx F_{Lc}$, when the number of velocity oscillations per the half period of $F_L(t)$ is significantly larger than unity. This expression for the frequency in the original units becomes $\Omega \approx 2\pi F_{ac}/a\eta$. Such a relation is anticipated for a decoupled vortex moving in the pinning potential with periodicity a.

5. ENHANCEMENT OF THE CRITICAL CURRENT DENSITY IN SUPERCONDUCTING/MAGNETIC MULTI-LAYERS

The polaronic mechanism of pinning is promising for achieving a high critical current. We propose using a superconducting (S) and magnetic (M) multilayer
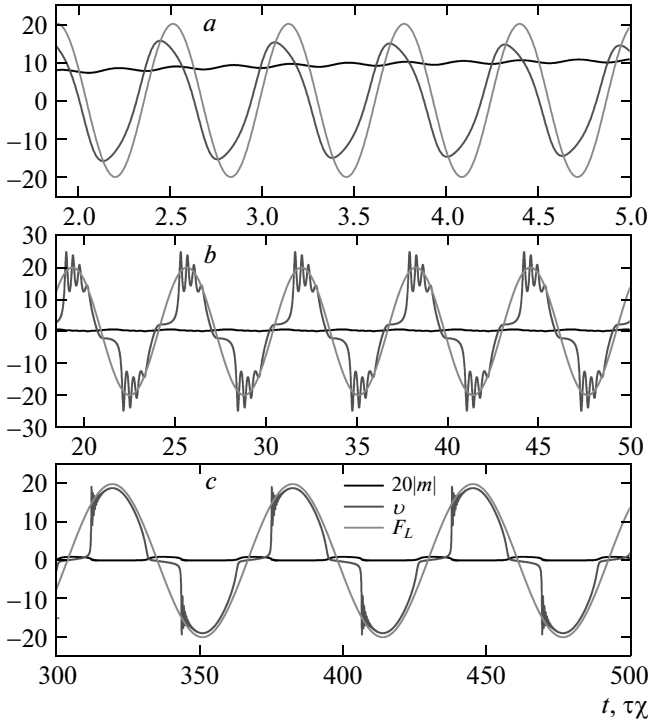
Fig. 6. Time evolution of the vortex velocity $v(t)$ and of magnetization $|m(t)|$ in the presence of the ac driving force $F_L(t) = F_{ac}\sin(\omega t)$ at several frequencies $\omega = 10$ (a), 1 (b), 0.1 (c). We take $F_{ac} = 20$ and $F_p = 20$
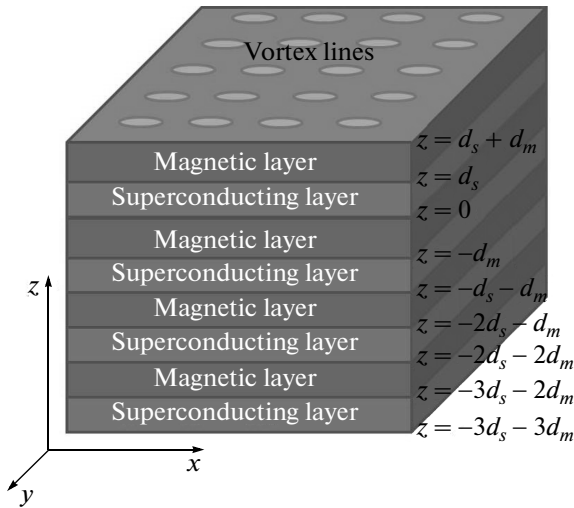

Fig. 7. Schematic view of a multi-layer structure consisting of alternating magnetic (M) layers (dark grey) with thickness d_m and superconducting (S) layers (light grey) with thickness d_s

structure shown in Fig. 7 for optimizing such a pinning mechanism [32]. To achieve a high critical current, the magnetic layers must have a slow relaxation of the magnetization. The magnetic layers must also have a high magnetic susceptibility at the working magnetic field to ensure a strong coupling between magnetic moments and vortices. In addition, the penetration depth of the superconducting layers must be small, such that the magnetization polarization varies rapidly in space.

The vortex lattice is induced inside the S layers under external magnetic fields. The vortex lattice moves in response to the Lorentz force when a transport current is present. In the quasistatic approximation, the motion of the vortex lattice is given by

$$\lambda^2 \nabla \times \nabla \times \mathbf{B} + \mathbf{B} = \Phi_0 \sum_i \delta\left[\mathbf{r} - \mathbf{r}_i(t)\right]\hat{\mathbf{z}}, \qquad (28)$$

where $\hat{\mathbf{z}}$ is the unit vector along the z axis and $\mathbf{r}_i(t) = \mathbf{r}_0 - \mathbf{v}t$ is the vortex i coordinate. The magnetic field inside the M layers is governed by the Maxwell equations

$$\nabla \times (\mathbf{B} - 4\pi\mathbf{M}) = 0, \quad \nabla \cdot \mathbf{B} = 0. \qquad (29)$$

The dependence of the magnetization $\mathbf{M}$ on $\mathbf{B}$ is determined by the material properties. With a strong field and in static case, $\mathbf{M}$ is a nonlinear function of $\mathbf{B}$ and generally can be expressed as

$$\mathbf{M}(\mathbf{r}) = \int dr^3 f[\mathbf{r} - \mathbf{r}', \mathbf{B}(\mathbf{r}')].$$

The characteristic length of the magnetic subsystem is much smaller than λ and we use the local approximation

$$f[\mathbf{r} - \mathbf{r}', \mathbf{B}(\mathbf{r}')] = \delta(\mathbf{r} - \mathbf{r}')f(\mathbf{B}(\mathbf{r}').$$

The induction $\mathbf{B}(\mathbf{r})$ has a component uniform in space, $\mathbf{B}_0$, and the nonuniform component $\tilde{\mathbf{B}}(\mathbf{r}) \ll \mathbf{B}_0$. Hence, the spatially nonuniform magnetization is

$$\tilde{\mathbf{M}}(\mathbf{r}) \approx \frac{\partial f(\mathbf{B}_0)}{\partial B_0}\tilde{\mathbf{B}}(\mathbf{r}) \equiv \chi_0(\mathbf{B}_0)\tilde{\mathbf{B}}(\mathbf{r}).$$

In what follows, we consider an isotropic magnetic subsystem characterized by a susceptibility $\chi_0(\mathbf{B}_0)$ at $\mathbf{B}_0$ in the static case. The magnetic field inside the M layer is determined by the equation $\nabla^2\tilde{\mathbf{B}} = 0$. Since only the spatially nonuniform components $\tilde{\mathbf{M}}$ and $\tilde{\mathbf{B}}$ are responsible for pinning, we focus on the nonuniform components in the calculations and omit the tilde. At the interface between the M and S layers, we use the standard boundary condition for the field B^z parallel to the z axis and the field $B^\parallel$ parallel to the interface:

$$B^z|_S = B^z|_M, \quad B^\parallel|_S = (1 - 4\pi\chi_0)B^\parallel|_M. \qquad (30)$$

Then we obtain the magnetic field inside the M layers:

$$B_m^z(G > 0, z) = \alpha \left[\exp(Gz') + \exp(-G(z'+d_m))\right] \times$$
$$\times \frac{\Phi_0 \exp\left(-iG_x v_x t\right)}{1 + \lambda^2 G^2}, \quad (31)$$

$$B_m^\parallel(G > 0, z) = i\alpha \left[\exp(Gz') - \exp(-G(z'+d_m))\right] \times$$
$$\times \frac{\Phi_0 \exp\left(-iG_x v_x t\right)}{1 + \lambda^2 G^2}, \quad (32)$$

$$\alpha = -\exp(d_m G)\left(-1 + \exp(d_s k_s)\right)\chi' \times$$
$$\times \left\{(1 - \chi')\left(\exp(d_s k_s) - \exp(G d_m)\right) + \right.$$
$$\left. + (1 + \chi')\left(1 - \exp(d_m G + d_s k_s)\right)\right\}^{-1},$$

with

$$z' = z - n(d_s + d_m), \quad k_s = \sqrt{\lambda^{-2} + G^2},$$
$$\chi' = (1 - 4\pi\chi_0)^{-1}k_s/G.$$

Here, n is the layer index and the vortex motion is assumed to be along the x direction. We consider a square lattice $\mathbf{G} = (m_x 2\pi/a, m_y 2\pi/a)$ with $a = \sqrt{\Phi_0/B_0}$ being the lattice constant and m_x and m_y integers.

We assume a relaxational dynamics for the M layers, $\mathbf{M}(\omega) = \chi(\omega)\mathbf{B}_m(\omega)$, with the dynamic susceptibility governed by a single relaxation time $\chi_0 \tau$ as in Eq. (10). In the steady state, we have

$$\mathbf{M}(\mathbf{G}, z, t) = \tau^{-1}\int_0^t \exp\frac{t' - t}{\chi_0 \tau}\mathbf{B}_m(\mathbf{G}, z, t')\, dt'. \quad (33)$$

For a slow relaxation of magnetization, $\mathbf{M}$ depends on the history of vortex motion and there is retardation between the time variation of the induced nonuniform magnetization and vortex motion. As a result, the magnetization exerts a drag force to the vortex, which is opposite to the driving force. The pinning force acting on a single vortex due to the induced magnetization in one M layer is given by

$$F_M = \partial_{r_0}\int dx\, dy \int_{-d_m}^0 dz \mathbf{M}\cdot\mathbf{B}_m,$$

which yields

$$F_M = \sum_G \left[1 - \exp\left(-2G d_m\right)\right] \times$$
$$\times \frac{2\alpha^2 \chi_0}{(1 + \lambda^2 G^2)^2 a^2}\frac{G v \chi_0 \tau \Phi_0^2}{1 + (G v \chi_0 \tau)^2}. \quad (34)$$

The I–V curve is determined by the equation of motion for the vortex $d_s \eta v = d_s F_L - F_M$ with the electric field $E = Bv/c$ and the Lorentz force $F_L = J\Phi_0/c$. We consider a realistic case where $a/2\pi \ll d_m, d_s$. Taking only the dominant contribution $G_x = 2\pi/a$ and $G_y = 0$ into account in the summation, we obtain the same equation as Eq. (15), but with a different parameter

$$F_p = \frac{\tau}{2\eta d_s}\left(\frac{1}{1 - 2\pi\chi_0}\right)^2 \frac{\chi_0^2 a \Phi_0^2}{\lambda^4 (2\pi)^3}, \quad (35)$$

after introducing the same dimensionless units as before.

Hysteresis is developed when $F_p \geq 8$. For typical parameters for an Nb superconductor, $\xi \approx \lambda \approx 40$ nm, $\rho_n \approx 10^{-6}\ \Omega\cdot$m and $a = 40$ nm at $B \approx 1$ T, and $\chi_0 = 0.05$, $F_p > 8$ requires $\chi_0 \tau > 1$ ps. For the relaxation time of the order of $\chi_0 \tau \approx 1\ \mu$s, the effective viscosity is enhanced by a factor of 10^6 compared to the bare BS one at $v < a/\chi_0 \tau$. The effective critical current density for the whole system is given by

$$J_c \approx \left(\frac{1}{2 - 4\pi\chi_0}\right)^2 \frac{\chi_0 c}{(2\pi)^4 \lambda^4}\frac{\Phi_0 a^2}{d_s + d_m}. \quad (36)$$

For $d_s = d_m = 100$ nm, we obtain $J_c \approx 10^9$ A/m^2. The retrapping current J_r is

$$J_r \approx \frac{1}{1 - 2\pi\chi_0}\sqrt{\frac{\eta a d_s}{\pi \tau}}\frac{ac}{\lambda^2 4\pi^2}\frac{1}{d_s + d_m}. \quad (37)$$

For the parameters used above and $\chi_0 \tau = 1\ \mu$s, we estimate $J_r \approx 2\cdot 10^6$ A/m^2.

We discuss the optimal materials for the S and M layers. Superconductors with a smaller λ are preferred because the critical current decreases as λ^{-4}. The smaller λ, the more nonuniform is the magnetic field distribution inside the M layers, and hence the stronger the pinning. The viscosity in the branch with a vortex polaron is proportional to τ while the critical current is independent of τ for sufficiently large τ. The slow magnetic dynamics can be realized in certain spin glasses, where the magnetization relaxation is governed by a broad spectrum of time scales, with the average time of the order of 0.1 μs [33, 34]. For CuMn$_{0.08}$, $\chi_0 \approx 0.002$ at $B = 1$ T [35]. We can enhance χ_0 by tuning the concentration of magnetic metal in alloys [36]. We can also use superparamagnets with τ as large as 1 s and with a huge χ_0 due to large magnetic moments in superparamagnets [37–39] and the recently synthesized cobalt-based and rare-earth-based single-chain magnets with $\chi_0 \approx 0.05$ at $B = 1$ T and 10^{-6} s $< \chi_0 \tau < 10^{-4}$ s [40–43].

We now discuss the optimal thickness of M and S layers. For $d_m \gg a$, we have

$$B_m(G > 0) \approx \exp(-2\pi d_m/a)$$

if $-d_m \ll z' \ll 0$ according to Eqs. (31) and (32). The magnetic induction and the magnetization are almost uniform in the lateral direction in the middle of the M layer. As a result, the pinning force becomes practically independent of d_m in this case. In other words, the pinning is effective only near the boundaries between S and M layers in the area of thickness of the order a. On the other hand, the Lorentz force is proportional d_s. Therefore, the effective critical current of the whole system J_c is proportional to $1/(d_s + d_m)$ as described by Eq. (36). Hence, the thinner both M and S layers, the higher is the critical current of the system.

The M/S multilayer structure is naturally realized in certain superconducting single crystals, such as $(RE)Ba_2Cu_3O_7$ [44, 45] and $RuSr_2GdCu_2O_8$ [46]. For $(RE)Ba_2Cu_3O_7$, magnetic RE ions interact weakly with superconducting electrons because they are positioned between the superconducting layers. They order at very low Néel temperatures of the order of $T_N \sim 1$ K. The polaronic mechanism is important at $T > T_N$, where spins are free. The London penetration depth of cuprate superconductors is large, $\lambda \approx 200$ nm, and hence the critical current is reduced significantly compared to that for the Nb multilayer structure, because J_c decreases as $1/\lambda^4$. Another natural realization is the recently discovered iron-based superconductors, such as $(RE)FeAsO_{1-x}F_x$, where RE ions are ordered antiferromagnetically below $T_N \sim 1$ K [47]. In $RuSr_2GdCu_2O_8$, the magnetic moments order ferromagnetically above T_c, and therefore the dominant enhancement of vortex viscosity is due to the radiation of magnons [23–25].

6. CONCLUSIONS

Vortices in magnetic superconductors polarize magnetic moments and become dressed and polaron-like. At low currents and a long spin relaxation time, the nonuniform polarization induced by vortices slows their motion at currents for which pinning by crystal lattice disorder becomes ineffective. As the current increases above the critical one, vortices release the nonuniform part of the polarization, and the velocity as well as the voltage in the I–V characteristics jump to much higher values. At a decreasing current, vortices are retrapped by polarized magnetic moments at the retrapping current which is smaller than the critical one. The results

of such a polaronic mechanism are in qualitative agreement with the experimental data [10, 15], but measurements of the I–V characteristics are needed to establish the quantitative agreement and confirm the validity of such a model for Er borocarbide. The polaronic mechanism should also operate in Gd and Tb borocarbides superconductors in the commensurate SDW phase and a strong effect can be present in Tm borocarbide above T_N.

We derive the response of the magnetic superconductors in the vortex state to the ac Lorentz force $F_L(t) = F_{ac}\sin(\omega t)$, taking the polaronic effect into account. At low amplitudes of the driving force F_{ac}, the dissipation in the system is suppressed due to the enhancement of the effective viscosity at low frequencies and due to formation of the magnetic pinning at high frequencies ω. In the adiabatic limit with low frequencies ω and a high amplitude of the driving force F_{ac}, the vortex and magnetic polarization form a vortex polaron when $F_L(t)$ is small. As F_L increases, the vortex polaron accelerates and at a threshold driving force it dissociates, i. e., the vortex motion and the magnetization relaxation decouple. As F_L decreases, the vortex is retrapped by the background of remnant magnetization and they again form a vortex polaron. This process repeats when $F_L(t)$ increases in the opposite direction. Remarkably, after dissociation, decoupled vortices move in the periodic potential induced by magnetization, which remains for some periods of time due to retardation of magnetization after the decoupling. At this stage, vortices oscillate with high frequencies determined by the amplitude of the Lorentz force at the instant of dissociation.

We propose fabricating multilayer system M/S where superconducting and magnetic layers can be optimized to achieve high critical current.

REFERENCES

1. L. N. Bulaevskii and S.-Z. Lin, Phys. Rev. Lett. **109**, 027001 (2012).

2. P. C. Canfield, P. L. Gammel, and D. J. Bishop, Phys. Today **51**, 40 (1998).

3. S. L. Bud'ko and P. C. Canfield, C. R. Physique **7**, 56 (2006).

4. L. C. Gupta, Adv. Phys. **55**, 691 (2006).

5. L. N. Bulaevskii, A. I. Buzdin, M. L. Kulic, and S. V. Panjukov, Adv. Phys. **34**, 175 (1985).

6. B. K. Cho, P. C. Canfield, L. L. Miller, D. C. Johnston, W. P. Beyermann, and A. Yatskar, Phys. Rev. B **52**, 3684 (1995).

7. P. Canfield, S. Bud'ko, and B. Cho, Physica C **262**, 249 (1996).

8. S. Choi, J. W. Lynn, D. Lopez, P. L. Gammel, P. C. Canfield, and S. L. Bud'ko, Phys. Rev. Lett. **87**, 107001 (2001).

9. H. Kawano-Furukawa, H. Takeshita, M. Ochiai et al., Phys. Rev. B **65**, 180508 (2002).

10. P. L. Gammel, B. Barber, D. Lopez et al., Phys. Rev. Lett. **84**, 2497 (2000).

11. H. Bluhm, S. E. Sebastian, J. W. Guikema, I. R. Fisher, and K. A. Moler, Phys. Rev. B **73**, 014514 (2006).

12. S. S. James, C. D. Dewhurst, S. B. Field et al., Phys. Rev. B **64**, 092512 (2001).

13. J. Appel, *Polarons, Solid State Physics*, ed. by F. Seitz and D. Turnbull, **21**, p. 193, Acad. Press, New York (1968).

14. I. S. Veschunov, L. Y. Vinnikov, S. L. Bud'ko, and P. C. Canfield, Phys. Rev. B **76**, 174506 (2007).

15. U. Yaron, P. L. Gammel, A. P. Ramirez et al., Nature **382**, 236 (1996).

16. M. Tachiki, H. Matsumoto, and H. Umezawa, Phys. Rev. B **20**, 1915 (1979).

17. K. E. Gray, Phys. Rev. B **27**, 4157 (1983).

18. A. I. Buzdin and L. N. Bulaevskii, Usp. Fiz. Nauk **149**, 45 (1986). [Sov. Phys. Usp. **29**, 412 (1986).]

19. S.-Z. Lin and L. N. Bulaevskii, Phys. Rev. B **86**, 014518 (2012).

20. E. I. Blount and C. M. Varma, Phys. Rev. Lett. **42**, 1079 (1979).

21. A. E. Koshelev and V. M. Vinokur, Phys. Rev. Lett. **73**, 3580 (1994).

22. R. Besseling, N. Kokubo, and P. H. Kes, Phys. Rev. Lett. **91**, 177002 (2003).

23. A. Shekhter, L. N. Bulaevskii, and C. D. Batista, Phys. Rev. Lett. **106**, 037001 (2011).

24. S. Z. Lin, L. N. Bulaevskii, and C. D. Batista, Phys. Rev. B **86**, 180506(R) (2012).

25. S.-Z. Lin and L. N. Bulaevskii, Phys. Rev. B **85**, 134508 (2012).

26. L. Bányai, Phys. Rev. Lett. **70**, 1674 (1993).

27. A. Hed and P. Freud, J. Non-Cryst. Sol. **2**, 484 (1970).

28. R. J. Cava, H. Takagi, H. W. Zandbergen et al., Nature **367**, 252 (1994).

29. P. Bonville, J. A. Hodges, C. Vaast et al., Z. Phys. B **101**, 511 (1996).

30. C. D. Dewhurst, R. A. Doyle, E. Zeldov, and D. McK. Paul, Phys. Rev. Lett. **82**, 827 (1999).

31. L. N. Bulaevskii and S.-Z. Lin, Phys. Rev. B **86**, 224513 (2012).

32. S.-Z. Lin and L. N. Bulaevskii, Phys. Rev. B **86**, 064523 (2012).

33. Y. J. Uemura, T. Yamazaki, D. R. Harshman, M. Senba, and E. J. Ansaldo, Phys. Rev. B **31**, 546 (1985).

34. K. Binder and A. P. Young, Rev. Mod. Phys. **58**, 801 (1986).

35. J. Prejean, M. Joliclerc, and P. Monod, J. Physique **41**, 427 (1980).

36. J. Kouvel, J. Phys. Chem. Sol. **21**, 57 (1961).

37. C. P. Bean and J. D. Livingston, J. Appl. Phys. **30**, S120 (1959).

38. R. B. Goldfarb and C. E. Patton, Phys. Rev. B **24**, 1360 (1981).

39. B. D. Cullity and C. D. Graham, *Introduction to Magnetic Materials*, Wiley-IEEE Press (2008).

40. A. Caneschi, D. Gatteschi, N. Lalioti et al., Angew. Chem. Int. Ed. **40**, 1760 (2001).

41. A. Caneschi, D. Gatteschi, N. Lalioti et al., Europhys. Lett. **58**, 771 (2002).

42. L. Bogani, C. Sangregorio, R. Sessoli, and D. Gatteschi, Angew. Chem. Int. Ed. **44**, 5817 (2005).

43. K. Bernot, L. Bogani, A. Caneschi, D. Gatteschi, and R. Sessoli, J. Amer. Chem. Soc. **128**, 7947 (2006).

44. P. H. Hor, R. L. Meng, Y. Q. Wang et al., Phys. Rev. Lett. **58**, 1891 (1987).

45. P. Allenspach, B. W. Lee, D. A. Gajewski et al., Z. Phys. B **96**, 455 (1995).

46. A. C. McLaughlin, W. Zhou, J. P. Attfield, A. N. Fitch, and J. L. Tallon, Phys. Rev. B **60**, 7512 (1999).

47. C. Wang, L. Li, S. Chi et al., Europhys. Lett. **83**, 67006 (2008).